OFDM Pulse Shaping for use in 5G Systems

Jaime J. Luque Quispe and Luís Geraldo P. Meloni

Abstract— **Currently new waveforms spectrally more efficient than the Orthogonal Frequency Division Multiplexing (OFDM) modulation are being studied by recent research projects for the development of the 5G physical layer. Although OFDM has powerful features such as implementation flexibility and robustness against channel selectivity and intersymbol interference (ISI), its use is not certain in the new emerging communication systems mainly due to its carrier frequency offset sensitivity, very large dynamic amplitude range, and high-power spectral sidelobes around active subcarriers eventually generating out-of-band emissions (OOBE) which in some cases cause intercarrier interference (ICI) among channels. These drawbacks limit its use in heterogeneous and densed 5G networks and in fragmented spectrum and cognitive radio scenarios where flexible use of spectrum is very important. This paper presents the analysis of the time-domain windowing technique applied to OFDM (W-OFDM) to deal with the OFDM OOBE problem. The effect of windowing is analytically derived and constraints are given on the window formats to guarantee the non significant signal-to-interference power ratio (SIR) and BER degradations caused by ISI and ICI. Numerical simulations are elaborated for a scenario based on 5-MHz 3GPP Long-Term Evolution (LTE) and multipath channel.**

Keywords— **OFDM, 5G, LTE, Pulse Shaping.**

I. INTRODUCTION

The traffic demand in wireless communications systems has been increasing exponentially over the past years. Nowadays, the challenges imposed by the requirements of the forthcoming 5G cellular technology make the development of new transmission techniques of paramount importance [1], [2]. This is motivating intense research work on new spectrally agile waveforms for higher data rates, higher user capacity and low latency that provide a flexible way to integrate the air interface with the other layers as well as to support different radio access technologies. On the other hand, enough contiguous spectrum to offer a broadband communication is not always available. In this regard, in order to achieve improved spectrum usage, some new modulation formats suited for 5G [3] [4], carrier aggregation and cognitive radio techniques for fragmented spectrum scenarios, have been some developments that address these challenges.

Orthogonal frequency division multiplexing (OFDM) is the modulation method adopted in 4G LTE cellular technology. The idea behind OFDM is the subdivision of a high rate serial data stream in a high number of low rate parallel data streams which modulates a group of baseband overlapped orthogonal subcarriers. As a consequence, a wideband frequency selective channel is reduced to various narrowband flat fading channels which makes OFDM robust against multipath fading and

Jaime J. Luque Quispe and Luís Geraldo P. Meloni¸ School of Electrical and Computer Engineering, University of Campinas, Campinas-SP, Brazil, E-mails: luque@decom.fee.unicamp.br, meloni@decom.fee.unicamp.br.

enables the use of simple equalizers to compensate the channel response. Further, OFDM offers high inmunity to channel delay spread and ISI using symbols with cyclic prefix (CP), it can be implemented very efficiently using Fast Fourier Transform (FFT) and inverse FFT algorithms, and supports adaptive data modulation.

However, OFDM is not free from constraints and drawbacks. Its poor spectral containment limits its use in densed networks and asynchronous communications, as well as in shared and fragmented spectrum scenarios. In OFDM, a rectangular pulse shape is used per subcarrier which results in high spectral sidelobes around each subcarrier and eventually in OOBE. The offset carrier frequency (CFO) may cause loss of orthogonality between subcarriers, an effect known as intercarrier interference (ICI), which represents the high sensitivity of OFDM to frequency synchronization errors [5]. Also, ISI and ICI are introduced into a received signal when CP is not sufficient to contain the time dispersion of the previous symbol. Aditionally, OFDM signals suffers from high peak-to-average power ratio (PAPR).

New technologies for 5G are envisioned to deliver higher data rates than existing systems and to support a high number of connected devices and heterogeneous data rate traffic with more stringent requirements in latency and energy efficiency. Given that OFDM assumes perfect synchronization between devices in the network and to the above drawbacks, its use in the 5G system is not taken for granted [3].

Some promising techniques for improving the performance of OFDM for 5G systems have been summarized in [4]. A dynamic deactivation of edge subcarriers offers a flexible way to shape the spectrum [6], although it is suitable for a non contiguous spectrum scenario, these guard bands jointly with CP decrease the spectral efficiency. Another way to reduce the spectral leakage is to filter the time domain OFDM signal. Nevertheless, in a fragmented spectrum scenario, filtering could be expensive to implement because separate filters have to be used for each fragment [7]. A method with very flexible application to CP-OFDM waveforms is pulse shaping, also known as windowing, where the OFDM symbols are reshaped in time domain with an appropriate window for smoothing the transitions between two consecutive symbols [6].

This paper addresses the impact of pulse shaping on OFDM spectral leakage reduction as well as its contribution on ISI and ICI interferences. The development of a mathematical model for OFDM waveforms is presented in section II. In section III, two formats of pulse shaping are presented and the OOBE supression using the power spectral density (PSD) is analyzed. Section IV focuses on analytic derivations of constraints for window formats to limit the ISI and ICI contributions when some samples of CP are used for windowing, as well as, the signal to interference power ratio (SIR) performance parameter

is obtained. Section V presents numerical simulations of SIR and BER performance for a scenario based on 5-MHz 3GPP Long-Term Evolution (LTE). Section VI is devoted to some conclusions.

II. SYSTEM MODEL

A N-subcarrier baseband continuous-time OFDM signal with arbitrary pulse shaping can be expressed as

$$x(t) = \sum_{l=-\infty}^{\infty} \sum_{k=0}^{N-1} S_{k,l} p(t - lT) e^{j2\pi f_k(t-lT)} \qquad (1)$$

where $j = \sqrt{-1}$, N is the IFFT length, f_k is the frequency of the k-th subcarrier, $p(t)$ is the time-limited pulse shaping function, T is the total symbol duration, and $S_{k,l}$ where $k = 0, 1, ..., N-1$, is the input data symbol sequence transmitted on the k-th subcarrier during the l-th OFDM symbol. We assume that $S_{k,l} \in \{S_{0,l}, S_{1,l}, ..., S_{N-1,l}\}$ is zero mean i.i.d. Also, a frequency spacing between two consecutive subcarriers, defined as $\Delta f = 1/T_N$, is specified to ensure orthogonality between all subcarriers over the useful symbol period T_N. As a consequence, the frequency separation between two arbitrary subcarrier frequencies f_{k_1} and f_{k_2} is defined as (2), where k_1 and k_2 denotes the k_1-th and k_2-th subcarriers respectively. If not satisfied, recovered subcarriers after the FFT at the receiver will be distorted due to ICI.

$$f_{k_1} - f_{k_2} = \frac{k_1 - k_2}{T_N} = (k_1 - k_2)\Delta f \qquad (2)$$

Generally a CP is appended at the begining of the symbol to absorb the channel delay spread. In that case, T_N is extended by T_{CP}, such that $T = T_{CP} + T_N$ as indicated in (1). If $x(t)$ is sampled at $t = nT_N/N$, where $n \in Z$ is the sample index, the discrete-time OFDM signal can be expressed as (3).

$$x[n] = \sum_{l=-\infty}^{\infty} \sum_{k=0}^{N-1} S_{k,l} p[n - lN_T] e^{j2\pi k(n-lN_T)/N} \qquad (3)$$

where N_{CP} and N_T are the number of samples for CP and total OFDM symbol respectively, so that $N_T = N_{CP} + N$.

The spectral containment of OFDM signal with arbitrary pulse shaping can be described using its PSD defined in (4).

$$PSD_x(f) = \frac{1}{T} \sum_{k=0}^{N-1} E\left[|S_{k,l}|^2\right] \left| P\left(f - \frac{k}{T_N}\right)\right|^2 \qquad (4)$$

where $P(f)$ is the fourier transform of $p(t)$.

The fast transition between two consecutive symbols caused by OFDM rectangular pulse shaping causes high power sidelobes around active subcarriers. This power can leak into the sidebands that are outside the OFDM spectrum, as well as to the subcarriers within the band. For this pulse format, the PSD is given by (5) and illustrated in Fig. 1 for a single subcarrier.

$$PSD_{x,rect} = T \sum_{k=0}^{N-1} E\left[|S_{k,l}|^2\right] \left| sinc\left[T\left(f - \frac{k}{T_N}\right)\right]\right|^2 \qquad (5)$$

The zero intersections and sidelobe peaks of the sinc function are moved when the CP is used [4] [6].
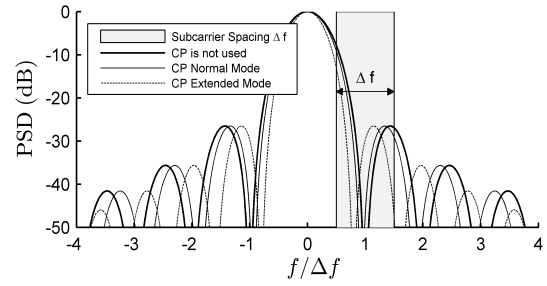
Fig. 1.   PSD of a single LTE 5-MHz OFDM subcarrier
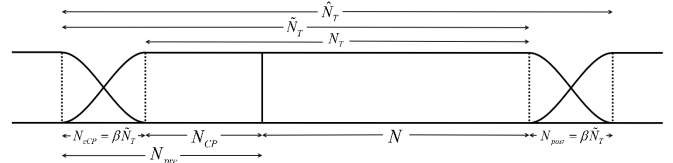
Fig. 2.   OFDM Pulse Shaping Format 1

III. IMPACT OF PULSE SHAPING ON SPECTRAL LEAKAGE REDUCTION

Pulse shaping [7] can reduce the spectral leakage exhibited in Fig. 1 making the PSD sidelobes of each subcarrier to decrease rapidly. The fast transitions at the edges of OFDM symbols are smoothed by multiplying the CP-OFDM samples with window samples aiming to generate lower sidelobes in frequency domain. The raised cosine window defined in (6) is very popular due to the flexible control of the number of samples in the transition region of the window. Where β is the roll off factor that controls the length of the transition region, and $\tilde{N}_T$ is the transmission period of a OFDM symbol.

$$p[n] = \begin{cases} \frac{1}{2} + \frac{1}{2}\cos\left[\pi\left(1 + \frac{n}{\beta\tilde{N}_T}\right)\right], & 0 \le n < \beta\tilde{N}_T \\ 1, & \beta\tilde{N}_T \le n < \tilde{N}_T \\ \frac{1}{2} + \frac{1}{2}\cos\left[\frac{\pi(n-\tilde{N}_T)}{\beta\tilde{N}_T}\right], & \tilde{N}_T \le n \le \tilde{N}_T(1+\beta) - 1 \end{cases}$$

$$(6)$$

Figures 2 and 3 illustrate two formats for discrete time window. In the first one the original symbol duration N_T is extended to $\tilde{N}_T$ in order to not distort the original N_{CP} samples of CP when pulse shape is applied. This format preserves the same inmunity to ISI, avoids extra processing at the receiver and avoids error vector magnitude (EVM) degradation. The resulting prefix denoted as N_{pre} is nothing more than the CP extended by $N_{eCP} = \beta\tilde{N}_T$ samples such that $N_{pre} = N_{CP} + N_{eCP}$. Also a cyclic postfix with $N_{post} = \beta\tilde{N}_T$ samples is appended at the end of the symbol which
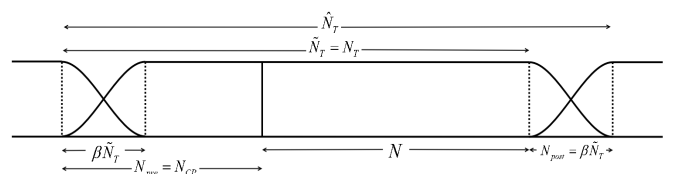
Fig. 3.   OFDM Pulse Shaping Format 2

means that the total window length is $N_{pre} + N + N_{post}$ which is denoted as $\hat{N}_T$. In order to decreases the bandwidth inefficiency due to time loss, two consecutive OFDM symbols are allowed to partially overlap in the rolloff N_{eCP} and N_{post} regions.

The second format can be used when it is not possible to extend the CP. In this case, some samples of CP could be used for the transition region without significative BER degradation, such that the OFDM transmision period is only N_T samples.

Using (4) and the Fourier transform of the raised cosine pulse in (7), the impact of β on spectral containment can be evaluated in terms of the mean relative interference power leakage ($\bar{P}_{leak}$) of a single subcarrier into a arbitrary subband Δf centered at n subcarriers positions as expressed by (8) [6]. The table I presents this parameter for some values of n.

$$|P_{rc}(f)| = \left| T_w \frac{\sin(\pi f T_w)}{\pi f T_w} \frac{\cos(\pi \beta f T_w)}{1 - (2\beta f T_w)^2} \right| \quad (7)$$

$$\bar{P}_{leak} = \frac{1}{P_{tot}} \int_{(n-0.5)\Delta f}^{(n+0.5)\Delta f} PSD_x(f) df \quad (8)$$

TABLE I
RELATIVE INTERFERENCE POWER $\bar{P}_{leak}$ FROM ONE 5-MHz LTE SUBCARRIER TO THE FOLLOWING SUBBANDS Δf USING RAISED COSINE WINDOW FORMAT 2

n	1	2	3	4
Normal CP Mode (144 T_{su})				
$\beta = 0$	6.9722	1.2165	0.5049	0.2763
$\beta = 0.15$	6.9993	1.0391	0.3277	0.1214
$\beta = 0.5$	5.6142	0.1531	0.002	0.0006
$\beta = 0.75$	4.2365	0.0129	0.0007	0.0001
Extended CP Mode (512 T_{su})				
$\beta = 0$	4.9222	0.8475	0.4832	0.3059
$\beta = 0.15$	4.8466	0.6779	0.2844	0.1066
$\beta = 0.5$	3.2540	0.0271	0.0019	0.0003
$\beta = 0.75$	2.0561	0.0042	0.0002	0.0001

$$T_{su} = 1/30720000 \text{ sec}$$

In Fig. 4 is illustrated the OFDM PSD for some values of β. The power of the sidelobes are reduced by increment of β, e.g. at frequency $f/\Delta f = 1$, for $\beta = 0$, 0.15, 0.5, and 0.75, the sidelobes are attenuated to -29.8 dB, -30.4 dB, -36.5 dB, and -46.1 dB respectively. In order for the transition windowing not to distort the N useful samples when window format 2 is used, β could be incremented as maximum a value such that $\beta \hat{N}_T \leq N_{CP}$. For extended CP, $N_T = 640$ samples and consequently a $\beta_{\max} = 0.2$ value could be specified without BER degradation in AWGN channel. Considering this maximum value of β, its effect on OOBE reduction is illustrated in Fig. 5.

IV. ISI AND ICI ANALYSIS

When CP is not sufficient to compensate the distortion due to channel delay spread, ISI and ICI ocurrs. In sequence, they
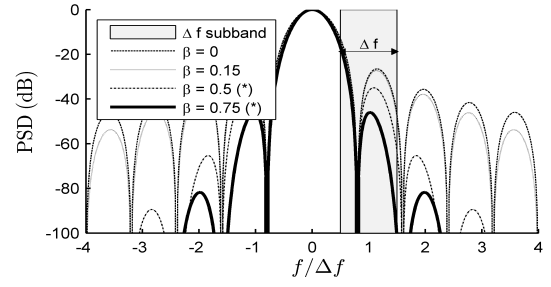
Fig. 4. Impact of β on the PSD of a single LTE 5-MHz W-OFDM subcarrier. Raised Cosine Window, Format 2. (*) some samples of the useful period T_N are used for transition region window.
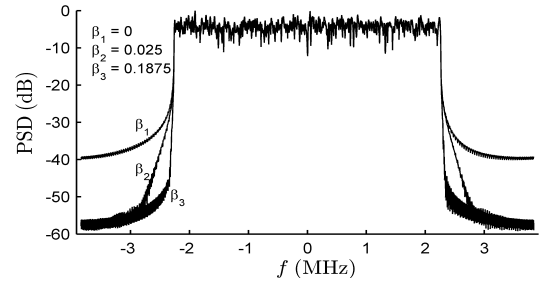
Fig. 5. PSD of a OFDM signal LTE 5-MHz carrier. Extended CP mode and window format 2.

are analyzed when delay spread immunity is reduced when window format 2 is used.

When two consecutive symbols overlap, the transmitted l-th OFDM symbol can be described by (9)

$$x^l[n] = \sum_{k=0}^{N-1} S_{k,l} p[n] e^{j2\pi kn/N}$$
$$+ \sum_{k=0}^{N-1} S_{k,l-1} p[n + \tilde{N}_T] e^{j2\pi k(n+\tilde{N}_T)/N} \quad (9)$$

where $n = -N_{pre}, -N_{pre}+1, ..., 0, 1, ..., N-1$ is the sample index, $\tilde{N}_T = N + N_{pre}$ is the length of transmitted OFDM symbol, $S_{k,l}$ and $S_{k,l-1}$ represent the data symbols in l-th and $(l-1)$-th OFDM symbols respectively. From (6) the second component in (9) is different of zero only in $n = -N_{pre}, -N_{pre}+1, ..., -N_{pre}+N_{post}-1$. To simplify the analysis, matrix representations are developed. Equation (9) can be expressed as

$$\mathbf{X}^l = \mathbf{T}(\mathbf{PGF}^H \mathbf{S}_{k,l} + \mathbf{EPGF}^H \mathbf{S}_{k,l-1}) \quad (10)$$

where $\mathbf{X}^l \in \mathbb{C}^{\tilde{N}_T}$ is the vector containing samples of the l-th transmitted OFDM symbol, $\mathbf{S}_{k,l}$ and $\mathbf{S}_{k,l-1} \in \mathbb{C}^N$, with $k = 0, 1, 2...N-1$ are vectors of subcarriers into l-th and $(l-1)$-th OFDM symbols respectively, $\mathbf{F} \in \mathbb{C}^{N \times N}$ is the N-point DFT matrix with entries $[F]_{r,c} = e^{-j2\pi rc/N}$, $r, c \in \{0, 1, ..., N-1\}$, $\mathbf{G} \in \mathbb{R}^{\hat{N}_T \times N}$ defined in (11) appends a prefix and postfix of N_{pre} and N_{post} samples respetively to both symbols in time domain, $\mathbf{P} \in \mathbb{N}^{\hat{N}_T \times \hat{N}_T}$ is a diagonal matrix whose diagonal elements are the coefficients of the transmit window as defined in (6), $\mathbf{E} \in \mathbb{N}^{\hat{N}_T \times \hat{N}_T}$ defined in (12) selects the last N_{post} samples of the $(l-1)$-th symbol to be added

(overlapped) to the first $\beta\tilde{N}_T$ samples of the lth symbol and by this reason it is set to $N_{post} = \beta\tilde{N}_T$. Finally, $\mathbf{T} \in \mathbb{N}^{\tilde{N}_T \times \hat{N}_T}$, defined in (13), selects the first $\tilde{N}_T$ samples of the overlaped symbol for transmission.

$$\mathbf{G} = \begin{bmatrix} 0_{Npre \ \mathrm{x} \ (N-Npre)} & I_{Npre} \\ & I_N & \\ I_{Npost} & 0_{Npost \ \mathrm{x} \ (N-Npost)} \end{bmatrix} \quad (11)$$

$$\mathbf{E} = \begin{bmatrix} 0_{Npost \ \mathrm{x} \ \tilde{N}_T} & I_{Npost} \\ & 0_{\tilde{N}_T \mathrm{x} \hat{N}_T} \end{bmatrix} \quad (12)$$

$$\mathbf{T} = \begin{bmatrix} I_{\tilde{N}_T} & 0_{\tilde{N}_T \mathrm{x} Npost} \end{bmatrix} \quad (13)$$

We consider a multipath channel with discrete time model during l-th symbol expressed by

$$h^l[n] = \sum_{m=0}^{L-1} \alpha^l[m]\delta[n-m] \quad (14)$$

where L is the number of paths, $\alpha[m]$ and m represents the complex amplitudes and propagation delays respectively. This results in time spreading of the $\mathbf{X}^l$ signal. If $L < \tilde{N}_T$, possible ISI on l-th symbol could occurs only from the $(l-1)$th symbol. When $\mathbf{X}^l$ is passed through (14), the received signal can be described as

$$\mathbf{Y}^l = \mathbf{H}^{(0)}\mathbf{X}^l + \mathbf{H}^{(1)}\mathbf{X}^{l-1} \quad (15)$$

where $\mathbf{H}^0$ and $\mathbf{H}^1$ are the channel matrices defined in (16) and (17) respectively.

$$H^{(0)} = \begin{bmatrix} h_0 & 0 & \cdots & \cdots & \cdots & \cdots & 0 \\ h_1 & h_0 & \ddots & \ddots & \ddots & \ddots & \vdots \\ \vdots & \ddots & \ddots & \ddots & \ddots & \ddots & \vdots \\ h_{L-1} & \cdots & \cdots & h_0 & 0 & \ddots & \vdots \\ 0 & h_{L-1} & \cdots & \cdots & h_0 & \ddots & \vdots \\ \vdots & \ddots & \ddots & \ddots & \ddots & \ddots & 0 \\ 0 & \cdots & 0 & h_{L-1} & \cdots & \cdots & h_0 \end{bmatrix} \quad (16)$$

$$H^{(1)} = \begin{bmatrix} 0 & \cdots & 0 & h_{L-1} & \cdots & h_1 \\ \vdots & \ddots & \ddots & \ddots & \ddots & \vdots \\ \vdots & \ddots & \ddots & \ddots & 0 & h_{L-1} \\ \vdots & \ddots & \ddots & \ddots & \ddots & 0 \\ \vdots & \ddots & \ddots & \ddots & \ddots & \vdots \\ 0 & \cdots & \cdots & \cdots & \cdots & 0 \end{bmatrix} \quad (17)$$

The first term in (15) contain the samples of l-th symbol convoluted with the channel where some of them are self distorted due to symbol overlaping. The second one is explicitly the ISI from the $(l-1)$-th symbol. However, commonly OFDM-based systems are designed with a CP longer than the maximum delay spread for different environments. In this case, the second term in (15) is discarded at the receiver as follows

$$\tilde{\mathbf{Y}}^l = \mathbf{R}\mathbf{Y}^l \quad (18)$$

where $\tilde{\mathbf{Y}}^l \in \mathbb{C}^N$ is the received OFDM symbol after N_{PRE} first samples are discarded and $\mathbf{R} \in \mathbb{N}^{N \times \tilde{N}_T}$ is defined as

$$\mathbf{R} \triangleq \begin{bmatrix} 0_{N \times \tilde{N}_T} & I_N \end{bmatrix} \quad (19)$$

Therefore the N received subcarriers obtained after FFT operation can be expressed as

$$\begin{aligned} \mathbf{Y}^l_{FFT} =& \mathbf{FRH}^{(0)}\mathbf{TPGF}^H\mathbf{S}_{k,l} \\ &+ \mathbf{FRH}^{(0)}\mathbf{TEPGF}^H\mathbf{S}_{k,l-1} \end{aligned} \quad (20)$$

Because some samples of CP are used for window, the self introduced ISI could not be absorbed by the remaining guard interval which results in ICI in frequency. When $\mathbf{S}_{k,l}$ and $\mathbf{S}_{k,l-1}$ are i.i.d., the SIR on an arbitrary received k' subcarrier can be expressed as

$$SIR_{k'} = \frac{\mu_{l,k=k'}}{\mu_{l,k\neq k'} + \lambda_{l-1,k}} \quad (21)$$

$$\mu_{l,k=k'} = \left| \mathbf{F}_{k'}\mathbf{RH}^{(0)}\mathbf{TPGU}_1\mathbf{F}^H\dot{\mathbf{S}}_{k,l} \right|^2 \quad (22)$$

$$\mu_{l,k\neq k'} = \left| \mathbf{F}_{k'}\mathbf{RH}^{(0)}\mathbf{TPGU}_2\mathbf{F}^H\dot{\mathbf{S}}_{k,l} \right|^2 \quad (23)$$

$$\lambda_{l-1,k} = \left| \mathbf{F}_{k'}\mathbf{RH}^{(0)}\mathbf{TEPGF}^H\dot{\mathbf{S}}_{k,l-1} \right|^2 \quad (24)$$

k and $k' \in \{0,1,...,N-1\}$, $\mathbf{F}_{k'}$ is the k'-th component of the FFT operation, U_1 and $U_2 \in \mathbb{N}^N$ are defined by (25) and (26) respectively, and $\dot{\mathbf{S}}_{k,l}$ and $\dot{\mathbf{S}}_{k,l-1}$ are defined as two arrays of one elements.

$$U_1[k] = \delta(k - k') \quad (25)$$

$$U_1[k] = 1 - \delta(k - k') \quad (26)$$

In (21), $\mu_{l,k=k'}$ represents the received power on k' subcarrier in the l-th symbol, $\mu_{l,k\neq k'}$ is the contribution of the other subcarriers in the same symbol, and $\lambda_{l-1,k}$ is the ICI from the $(l-1)$ symbol.

The $\tilde{\mathbf{Y}}^l$ can still contain ISI from $\mathbf{X}^{l-1}$ if the time spread of the first $\beta\tilde{N}_T$ samples of $\mathbf{X}^l$ in (10) can not be absorbed by the remaining non-distorted CP. For a channel with L paths and a window with roll-off length $\beta\tilde{N}_T$ samples, the time spreading length of the transmitted overlapped samples is

$$N_{spread} = \beta\tilde{N}_T + L - 1 \quad (27)$$

Therefore, if $N_{pre} - \beta\tilde{N}_T \geq L-1$ neither ISI nor ICI ocurrs, otherwise the $\beta\tilde{N}_T + L - 1 - N_{PRE}$ samples not absorbed by CP will distort the N useful samples and will cause the loss of orthogonality between received subcarriers after FFT.

V. NUMERICAL RESULTS

The performance of W-OFDM is analyzed in terms of SIR and BER degradations caused by ISI and ICI. We consider the 5-MHz LTE scheme with 16-QAM and 64-QAM subcarrier mapping. In LTE, the OFDM frame is subdivided into 20 slots of 0.5 ms and each slot has a number of symbols which depends of the CP mode. They are defined two CP modes, the normal CP of 4.7us and the extended CP of 16.7us, which subdivides each slot in 7 and 6 symbols respectively. The useful symbol duration T_N is 66.7us and the subcarrier frequency separation is 15 KHz. For 5-MHz scheme, the IFFT
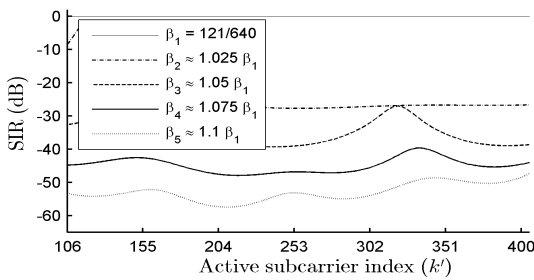
Fig. 6.   Normalized SIR on active subcarriers of a LTE 5MHz carrier for different window roll-off lengths. Extended CP mode and window format 2.
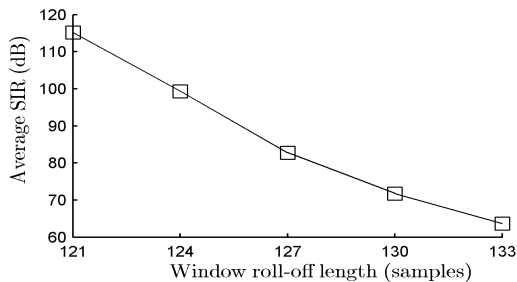
Fig. 7.   Average SIR over all active subcarriers for different window roll-off lengths

uses 512 points and 25 resource blocks (RBs). Each RB is composed by 12 subcarriers representing a useful bandidwidth of 4.5 MHz (300 subcarriers) whith 0.25 MHz of guard band at the sides of the spectrum. The sample frequency is 7.68 MHz, the normal CP has 36 samples and the extended CP has 128 samples.

A. Signal to interference ratio

In Fig. 6, the normalized SIR on 300 useful subcarriers is depicted. As example, a multipath channel width $L = 9$ taps is considered and different values of β are chosen. The result for β_1 confirms (27) as just only sample on useful symbol is contaminated with ISI and FFT output is constant. As β increases, more distortion ocurrs in the other subcarriers.

Also, the average SIR over all subcarriers as function of β is illustrated in Fig. 7. For $N_{PRE} = 128$ and $N_T = 640$, the delay spread is perfectly absorbed by CP when $\beta \tilde{N}_T \leq N_{PRE} - (L + 1)$, otherwise the average SIR is degradated as β is increased. Even if ISI occurs, its effect may be limited because the powers of the OFDM symbols arriving from longer delay paths are smaller than those arriving first and the power contribution of last N_{post} (delayed) samples of the $(l - 1)$-th symbol are limited by the decreasing region of the window.

B. BER performance

The fragmented spectrum scenario shown in Fig. 8 will be considered for BER performance of W-OFDM. The 25 RBs are divided as follows, 2 RBs are used for a desired CP-OFDM transmission (A), 19 RBs are used by an CP-OFDM inteferer (B) with pulse shaping option and 4 RBs
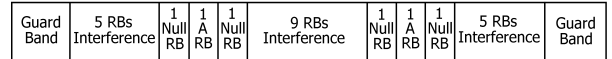
Fig. 8.   A 5-MHz non contiguous spectrum band
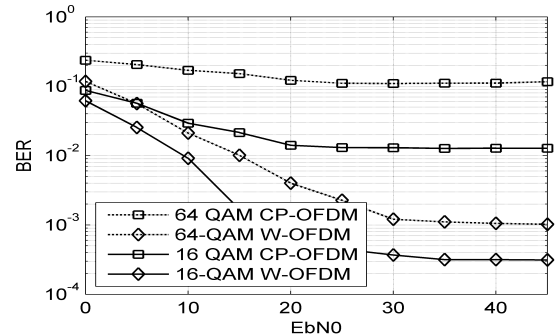
Fig. 9.   BER performance of W-OFDM in spectrum fragmented LTE 5-MHz scenario

have nulls subcarriers. The power of B is specified to be 5 dB above in relation to A and with a doppler shift of $0.5\Delta f$. The W-OFDM interferer version (format 2) uses 40 samples in window transition and both transmitters use extended CP. The BER is depicted in figure 9 for 16 and 64 QAM carrier modulations.

VI. CONCLUSION

This work has analyzed the ability of the pulse shaping technique to supress the OOBE aiming to increase the spectral containment of OFDM waveform and avoids interchannel interference. Also, were presented two window formats, where one exploits the existent CP and the other extends some samples to the OFDM symbol for smoothing. Mathematical expressions to evaluate the impact of pulse shaping on ICI and ISI were analytically derived and contraints to guarantee the non signiticant SIR degradation were obtained. Numerical simulations were performed to investigate the performance of W-OFDM in a fragmented spectrum scenario.

REFERENCES

[1] S. Talwar, D. Choudhury, K. Dimou, E. Aryafar, B. Bangerter and K. Stewart, "Enabling technologies and architectures for 5G wireless," *IEEE MTT-S International Microwave Symposium*, pp.1-4, June 2014.

[2] G. Wunder, P. Jung, M. Kasparick and T. Wild, "5GNOW: non-orthogonal, asynchronous waveforms for future mobile applications,", *IEEE Communications Magazine*, vol.52, no.2, pp.97-105, Feb. 2014.

[3] P. Banelli, S. Buzzi, G. Colavolpe, A. Modenini, F.Rusek, A. Ugolini, "Modulation Formats and Waveforms for 5G Networks: Who Will Be the Heir of OFDM?: An overview of alternative modulation schemes for improved spectral efficiency," *IEEE Signal Processing Magazine*, vol.31, no.6, pp.80,93, Nov. 2014.

[4] A.E. Loulou, S.A. Gorgani, and M. Renfors, "Enhanced OFDM techniques for fragmented spectrum use," *Future Network and Mobile Summit*, pp.1,10, July 2013.

[5] N.C. Beaulieu and T. Peng, "On the effects of receiver windowing on OFDM performance in the presence of carrier frequency offset," *IEEE Transactions on Wireless Comm.*, v.6, no.1, pp.202,209, Jan. 2007.

[6] T. Weiss, J. Hillenbrand, A. Krohn and F.K. Jondral, "Mutual interference in OFDM-based spectrum pooling systems," *IEEE Vehicular Technology Conference*. v.4, pp.1873,1877, May 2004.

[7] E. Bala, L. Jialing, and Y. Rui, "Shaping Spectral Leakage: A Novel Low-Complexity Transceiver Architecture for Cognitive Radio," *IEEE Vehicular Technology Magazine*, v.8, no.3, pp.38,46, Sept. 2013.